An Efficient Finite Element Method for Nonconvex Waveguide Based on Hermitian Polynomials

MOSHE ISRAEL, MEMBER, IEEE, AND RUTH MINIOWITZ

Abstract —An efficient finite element method (FEM) in waveguide analysis is described. The method uses Hermitian polynomials to interpolate the field component (E_z or H_z) and some of its derivatives at the nodal points, rather than the field components, as in the Lagrangian interpolation case. Element matrices, for a standard triangle, are given for third- and fifth-degree Hermitian polynomials. The appropriate transformations that relate the element matrices of a general triangle to the standard triangle element have been derived. Compared to the broadly used Lagrangian interpolation FEM, the Hermitian FEM has the following advantages:

1) a significant reduction of the matrix order needed to compute the eigenvalues and eigenfunctions;
2) smooth axial components (E_z or H_z) and continuous transverse field components;
3) low-cost refinement of the mesh near nonconvex corners of the waveguide.

These advantages are illustrated by comparing the FEM, with Hermitian polynomials solution, to other solutions for rectangular and ridged waveguides.

I. Introduction

IN DESIGNING waveguide devices, it is helpful to know the complete eigenvalue spectrum and the corresponding field solution. There are several approaches to solve waveguide problems (see, for example, [1]–[4]). The finite element method (FEM) [4] is a versatile method that we consider in this paper.

The first-order polynomial FEM is a broadly used method [3]. However, the method is uneconomical for accurate field computation requirements; consequently, most works using first-order polynomials concentrate on finding the eigenvalue spectrum, rather than the modal field. In contrast, the high-order Lagrangian polynomials FEM for triangular elements [4, pp. 88–90], when applied to convex waveguides, leads to substantial saving in computer storage and time. However, when sharp corners exist, the field singularities at these corners cause difficulties in obtaining a rapidly converging solution. In fact, numerical experiments relating to singularities in transmission lines [7] indicate that when the triangular mesh is refined, the convergence is only marginally improved for the higher order polynomials. Although the variational analysis given in [1] is efficient in the singular case, the analysis described there is specific to ridged waveguides. Unlike the variational analysis, the FEM has the advantage of being appropriate to an arbitrary waveguide shape.

In this paper we elaborate on the Hermitian polynomials and demonstrate their usefulness as far as efficiency is concerned. The efficiency mainly stems from the continuity requirements, not only on the function E_z or H_z, as in the Lagrangian case, but also on the first- and possibly second-order derivatives. In fact, these requirements reduce the order of the matrix eigenvalue problem. With this reduction, one is able to work with higher order polynomials with a cost similar to that of Lagrangian lower order polynomials. As an example [5, p. 85] if we consider a square which has been partitioned into $2n^2$ right-angle triangles, the matrix order corresponding to Lagrangian third-degree polynomials is about $9n^2$. An interpolation with third-degree Hermitian polynomials which imposes continuous first-order derivatives at the nodes reduces the order to about $5n^2$, but gives an error similar to the case with Lagrangian third-order polynomials. If we use reduced fifth-order Hermitian polynomials and require first and second continuous derivatives, the resulting matrix order is approximately only about $6n^2$. This significant reduction in the number of free parameters allows working with high-order polynomials when grid refinements are necessary, as in the case of sharp corners. The use of fifth-degree Hermitian polynomials has the additional advantage that it is possible to find an approximate solution which belongs to C^1. This fact will cause the field components to be continuous and the field lines to be smooth.

In comparison to the advantages mentioned, the disadvantage when using Hermitian polynomials is the inconvenience in the rather lengthy mathematical expressions involved. The problem of performing the appropriate integrations of these expressions over a single triangle is a discouraging stage. To overcome this difficulty, we have performed the integrations analytically for a standard triangle for third- and fifth-degree polynomials. The results are tabulated in Appendix II. We have also derived simple transformations that express the required information on a general triangle in terms of the standard triangle. Using these transformations and tables, the FEM with Hermitian polynomials is easily and effectively implemented.

Manuscript received March 23, 1987; revised June 29, 1987.
The authors are with the Electromagnetics Department, RAFAEL, P.O. Box 2250, Haifa 31021, Israel.
IEEE Log Number 8716593.

0018-9480/87/1100-1019$01.00

II. Variational Formulation

The axial field components in propagating modes of a uniform, perfectly conducting waveguide satisfy the Helmholtz equation

$$\left(\nabla^2 + k_T^2\right)\tilde{u} = 0 \tag{1}$$

where k_T is the cutoff wavenumber,

$$\nabla^2 = \frac{\partial^2}{\partial x^2} + \frac{\partial^2}{\partial y^2}$$

and $\tilde{u}$ stands for the axial field components $\boldsymbol{E}_z$ or $\boldsymbol{H}_z$ for TM or TE modes, respectively.

For TE modes, (1) is subject to Neumann boundary conditions, and for TM modes it is subject to Dirichlet boundary conditions. The FEM uses a variational formulation in which the functional

$$I(\tilde{u}) = \frac{1}{2}\int\int\left\{(\nabla\tilde{u})^2 - k_T^2\cdot\tilde{u}^2\right\}dx\,dy \tag{2}$$

is stationary.

While the Dirichlet boundary conditions should be imposed on the trial function, $\tilde{u}$, the Neumann boundary conditions are natural and it should not necessarily be imposed.

We construct an approximate solution that can be written as follows:

$$\tilde{u} = \sum_i \tilde{F}_i\tilde{\beta}_i. \tag{3}$$

This solution is a combination of trial functions $\tilde{\beta}_i(x, y)$; the $\tilde{F}_i$'s are parameters representing the values of the solution and its derivatives at mesh points.

If one substitutes (3) into (2), one obtains

$$I(\tilde{F}) = \frac{1}{2}\sum_i\sum_j \tilde{F}_i\tilde{F}_j\int\int\nabla\tilde{\beta}_i\nabla\tilde{\beta}_j\,dx\,dy - \frac{k_T^2}{2}\sum_i\sum_j\tilde{F}_i\tilde{F}_j\int\int\tilde{\beta}_i\tilde{\beta}_j\,dx\,dy. \tag{4}$$

Denoting by $\tilde{\boldsymbol{F}}$ the column vector of the values $\tilde{F}_i$, (4) can be written in matrix form as follows:

$$I(\tilde{F}) = \frac{1}{2}\tilde{\boldsymbol{F}}^T\tilde{\boldsymbol{S}}\tilde{\boldsymbol{F}} - \frac{k_T^2}{2}\tilde{\boldsymbol{F}}^T\tilde{\boldsymbol{T}}\tilde{\boldsymbol{F}} \tag{5}$$

where the elements of the square matrices $\tilde{\boldsymbol{T}}$ and $\tilde{\boldsymbol{S}}$ are given by

$$\tilde{T}_{ij} = \int\int\tilde{\beta}_i\tilde{\beta}_j\,dx\,dy$$
$$\tilde{S}_{ij} = \int\int\nabla\tilde{\beta}_i\nabla\tilde{\beta}_j\,dx\,dy. \tag{6}$$

These matrices are often referred to as mass and stiffness matrices, respectively.

In practical computations, we build first the corresponding $\boldsymbol{T}$ and $\boldsymbol{S}$ matrices for each triangle and then assemble the matrices to obtain the global matrices $\tilde{\boldsymbol{T}}$ and $\tilde{\boldsymbol{S}}$. This step is fully described elsewhere [4, pp. 16–32].

III. Hermitian Approximation Polynomials

Dividing the waveguide cross section into triangles, we approximate the axial field components for each triangle by

$$u = \sum_i F_i\beta_i \tag{7}$$

and similar to (4) and (5) we define the matrices $\boldsymbol{T}$ and $\boldsymbol{S}$.

The following transformation will map a triangle in the xy plane with vertices at $P_1(x_1, y_1)$, $P_2(x_2, y_2)$, and $P_3(x_3, y_3)$ onto the standard triangle $\Pi_1(1.,0.)$, $\Pi_2(0.,1.)$, and $\Pi_3(0.,0.)$ in the p_1p_2 plane:

$$x = x_3 + \xi_{13}p_1 + \xi_{23}p_2$$
$$y = y_3 + \eta_{13}p_1 + \eta_{23}p_2$$

where $\xi_{km} = x_k - x_m$ and $\eta_{km} = y_k - y_m$.

Since this transformation is always possible, it is convenient to develop first the formulation for a standard triangle and then to transform the result to a general triangle. This procedure is particularly efficient when the $\boldsymbol{T}$ and $\boldsymbol{S}$ matrices have to be computed for a general triangle.

In order to distinguish between the computations in the xy plane and those in the p_1p_2 plane, we shall denote the solution (7) in the p_1p_2 plane by

$$u = \sum_{i=1}^{N} G_i\alpha_i. \tag{8}$$

Let us consider first the third-order polynomials. These polynomials have ten coefficients (G_i) corresponding to the function values at the vertices and centroid and to the first partial derivatives at the vertices. Denoting the function values by u_1, u_2, and u_3 at the vertices 1, 2, and 3, respectively, and the value at the centroid by u_4, the coefficients G_i will be defined as follows:

$$G_i = u_i, \qquad i = 1,\ldots,4$$
$$G_{i+4} = \frac{\partial u_i}{\partial p_1} \qquad G_{i+7} = \frac{\partial u_i}{\partial p_2}, \qquad i = 1,2,3. \tag{9}$$

Explicit expressions of the polynomials α_i in terms of p_1, p_2 for the standard triangle are given in Appendix I. It is worth noting that the function u is uniquely interpolated along a side of a triangle. Consequently, a unique u will result on a common side of two triangles. This means that the interpolating function $\tilde{u}$ is continuous over the triangular network and therefore has C^0 continuity. Note that the transverse field components, given by the derivatives of $\tilde{u}$, are generally not continuous along the triangle sides.

A fifth-order polynomial has in general 21 coefficients to be determined. Matching the function and its first- and second-order derivatives gives 18 constraints. Here, the three remaining constraints are obtained by requiring that the normal derivatives u_n be reduced to a third-degree polynomial along each side of the triangle. It may be shown [6, pp. 49–50] that in this case the partial derivatives u_x and u_y are interpolated by a unique function along each triangle side and therefore $\tilde{u}$ has C^1 continuity.

Denoting

$$G_i = u_i \qquad G_{i+3} = \frac{\partial u_i}{\partial p_1} \qquad G_{i+6} = \frac{\partial u_i}{\partial p_2}$$

$$G_{i+9} = \frac{\partial^2 u_i}{\partial p_1 \partial p_2} \qquad G_{i+12} = \frac{\partial^2 u_i}{\partial p_1^2} \qquad G_{i+15} = \frac{\partial^2 u_i}{\partial p_2^2}, \qquad i=1,2,3 \tag{10}$$

we give explicit expressions of the polynomials α_i in terms of p_1 and p_2 for the standard triangle [6, p. 50] in Appendix I. When the standard triangle is transformed onto a general triangle, the normal to a side of the triangle will not generally be transformed onto the normal of the transformed side; consequently, the C^1 continuity may be destroyed. To preserve the C^1 property, it is essential to restrict the mesh elements to right-angle triangles (not necessarily isosceles) so that if two right-angle triangles share a hypotenuse they form a rectangle. We also require that the standard triangle's hypotenuse be transformed onto the triangle's hypotenuse. In this case, the normal to the hypotenuse of the standard triangle will be mapped onto the median to the triangle's hypotenuse. Consequently, along each common side of two triangles the derivative, in a unique direction of either the median or the normal to that side, reduces to a third-order polynomial and therefore is uniquely determined. Taking into account the uniqueness of the derivatives along the side direction, we conclude that the C^1 property is preserved. This implies continuity of all field components across the waveguide.

IV. Transformations from Standard to General Triangle

Considering now a general triangle, we first treat the third-degree polynomials. Recalling (7),

$$u = \sum_{i=1}^{10} F_i \beta_i$$

we define

$$F_i = u_i, \qquad i=1,\dots,4$$

$$F_{i+4} = \frac{\partial u_i}{\partial x} \qquad F_{i+7} = \frac{\partial u_i}{\partial y}, \qquad i=1,2,3. \tag{11}$$

Applying the chain rule and using (7), (8), (9), and (11), we obtain

$$\beta_i = \alpha_i, \qquad i=1,\dots,4$$

$$\beta_{i+4} = \xi_{13}\alpha_{i+4} + \xi_{23}\alpha_{i+7}$$

$$\beta_{i+7} = \eta_{13}\alpha_{i+4} + \eta_{23}\alpha_{i+7}, \qquad i=1,2,3. \tag{12}$$

Similarly, for fifth-degree polynomials, we have

$$u = \sum_{i=1}^{18} F_i \beta_i$$

$$F_i = u_i \qquad F_{i+3} = \frac{\partial u_i}{\partial x} \qquad F_{i+6} = \frac{\partial u_i}{\partial y}, \qquad i=1,2,3$$

$$F_{i+9} = \frac{\partial^2 u_i}{\partial x \partial y} \qquad F_{i+12} = \frac{\partial^2 u_i}{\partial x^2} \qquad F_{i+15} = \frac{\partial^2 u_i}{\partial y^2}. \tag{13}$$

Using the chain rule and (10), we obtain

$$\beta_i = \alpha_i, \qquad i=1,2,3$$

$$\beta_{i+3} = \xi_{13}\alpha_{i+3} + \xi_{23}\alpha_{i+6}$$

$$\beta_{i+6} = \eta_{13}\alpha_{i+3} + \eta_{23}\alpha_{i+6}$$

$$\beta_{i+9} = 2\cdot\xi_{13}\eta_{13}\alpha_{i+12} + 2\cdot\xi_{23}\eta_{23}\alpha_{i+15} + (\xi_{23}\eta_{13} + \xi_{13}\eta_{23})\alpha_{i+9}$$

$$\beta_{i+12} = \xi_{13}^2\alpha_{i+12} + \xi_{23}^2\alpha_{i+15} + \xi_{13}\xi_{23}\alpha_{i+9}$$

$$\beta_{i+15} = \eta_{13}^2\alpha_{i+12} + \eta_{23}^2\alpha_{i+15} + \eta_{13}\eta_{23}\alpha_{i+9}. \tag{14}$$

Either (14) or (12) may be abbreviated

$$\beta_i = \sum_{j=1}^{N} e_{ij}\alpha_j \tag{15}$$

where

$$N = \begin{cases} 10 \text{ - cubic case} \\ 18 \text{ - quintic case.} \end{cases}$$

The quantities e_{ij} are defined by (12) or (14) for the third- and fifth-degree cases, respectively.

Substituting the expression (15) into the first equation in (6), we obtain

$$T_{ij} = 2\cdot A \sum_{k=1}^{N} \sum_{m=1}^{N} e_{ik}e_{jm}T'_{km} \tag{16}$$

where T'_{jk} is an element of the mass matrix for the standard triangle and A is the area of the triangle. To obtain a transformation for S we follow [4 pp. 81–82] and define

$$Q_{ij}^{(1)} = \iint \frac{\partial \alpha_i}{\partial p_2}\cdot\frac{\partial \alpha_j}{\partial p_2}\, dp_1\, dp_2 \tag{17a}$$

$$Q_{ij}^{(2)} = \iint \frac{\partial \alpha_i}{\partial p_1}\cdot\frac{\partial \alpha_j}{\partial p_1}\, dp_1\, dp_2 \tag{17b}$$

$$Q_{ij}^{(3)} = \iint \left(\frac{\partial \alpha_i}{\partial p_1} - \frac{\partial \alpha_i}{\partial p_2}\right)\left(\frac{\partial \alpha_j}{\partial p_1} - \frac{\partial \alpha_j}{\partial p_2}\right) dp_1\, dp_2 \tag{17c}$$

to obtain

$$S'_{ij} = \sum_{k=1}^{3} Q_{ij}^{(k)}\cot\theta_k \tag{18}$$

where θ_k is the included angle at vertex k, and

$$S'_{ij} = \iint \left(\frac{\partial \alpha_i}{\partial x}\cdot\frac{\partial \alpha_j}{\partial x} + \frac{\partial \alpha_i}{\partial y}\cdot\frac{\partial \alpha_j}{\partial y}\right) dx\, dy. \tag{19}$$

Again, using the second equation in (6), we obtain

$$S_{ij} = \sum_{k=1}^{N} \sum_{m=1}^{N} e_{ik} e_{jm} S'_{km}. \tag{20}$$

Employing a special code, the matrices $\boldsymbol{T}'$ and $\boldsymbol{Q}^{(k)}$ have been evaluated analytically and the results are tabulated in Appendix II. Using these tables and (16)–(19), the $\boldsymbol{T}$ and $\boldsymbol{S}$ matrices of any triangle can be accurately and effectively constructed.

As mentioned earlier, the global mass and stiffness matrices are obtained by assembling the triangle elements S_{ij} and T_{ij}.

V. Boundary Conditions

When using Hermitian polynomials, it is often necessary to impose conditions on the derivatives of the function $\tilde{u}$ at the boundaries. Considering first the Dirichlet boundary conditions, we note that the condition $\tilde{u} = 0$ along a segment implies that all the derivatives in the direction of the segment vanish. If the direction is given by $\eta = (\eta_x, \eta_y)$, then

$$\tilde{u}'_\eta = \tilde{u}_x \eta_x + \tilde{u}_y \eta_y = 0. \tag{21}$$

Similarly, the second-order derivatives are given by

$$\tilde{u}''_{\eta\eta} = \tilde{u}_{xx} \cdot \eta_x^2 + 2 \cdot \tilde{u}_{xy} \cdot \eta_x \cdot \eta_y + \tilde{u}_{yy} \cdot \eta_y^2 = 0. \tag{22}$$

We denote by $\tilde{\boldsymbol{F}}_d$ a vector with elements describing the values of $\tilde{u}$ and its partial derivatives at the nodes of the entire mesh. Equations (21) and (22) represent dependence between elements of $\tilde{\boldsymbol{F}}_d$.

Next, we define a vector $\tilde{\boldsymbol{F}}_I$ which includes that part of $\tilde{\boldsymbol{F}}_d$ consisting only of the independent elements. Then, it follows that

$$\tilde{\boldsymbol{F}}_I = \boldsymbol{C} \tilde{\boldsymbol{F}}_d \tag{23}$$

where $\boldsymbol{C}$ is a matrix readily obtained from (21) and (22). The global matrices $\tilde{\boldsymbol{T}}_I$ and $\tilde{\boldsymbol{S}}_I$ corresponding to the independent parameters may be obtained by computing first the matrices $\tilde{\boldsymbol{T}}_d$ and $\tilde{\boldsymbol{S}}_d$ corresponding to the dependent vector $\tilde{\boldsymbol{F}}_d$; then by using (5) and (23) one may obtain the desired result

$$\tilde{\boldsymbol{T}}_I = \boldsymbol{C}^T \tilde{\boldsymbol{T}}_D \boldsymbol{C}$$
$$\tilde{\boldsymbol{S}}_I = \boldsymbol{C}^T \tilde{\boldsymbol{S}}_D \boldsymbol{C}. \tag{24}$$

The Neumann boundary conditions are natural and it is not necessary to impose them at the boundaries. However, including the conditions explicitly will result in a reduction in the order of $\tilde{\boldsymbol{T}}_I$ and $\tilde{\boldsymbol{S}}_I$. This process will increase the functional value (2), and in this sense the approximate solution is less accurate. However, many examples that we have performed indicate that the reduction of order usually compensates for the loss in accuracy. Denoting by $\xi = (\xi_x, \xi_y)$ the normal to the segment, we obtain the following conditions:

$$\tilde{u}'_\xi = \tilde{u}_x \xi_x + \tilde{u}_y \xi_y = 0 \tag{25}$$

$$\tilde{u}''_{\xi\eta} = \tilde{u}_{xx} \xi_x \eta_x + \tilde{u}_{xy} (\xi_y \eta_x + \xi_x \eta_y) + \tilde{u}_{yy} \xi_y \eta_y = 0. \tag{26}$$

The matrices $\tilde{\boldsymbol{T}}_I, \tilde{\boldsymbol{S}}_I$ will then be computed from (24) with the appropriate matrix $\boldsymbol{C}$.

TABLE I
Comparison between TE_{10}-Mode Cutoff Wavelength in a Rectangular Waveguide with Imposed Boundary Conditions

m	n	$\log\lvert\lambda_{HI}-\lambda_{EX}\rvert$	$\log\lvert\lambda_{L}-\lambda_{EX}\rvert$
8	34	-4.9	
8	49		-3.6
18	70	-6.2	
18	100		-4.6
32	114	-7.1	

TABLE II
Comparison between TE_{10}-Mode Cutoff Wavelength in a Rectangular Waveguide with Free Boundary Conditions

m	n	$\log\lvert\lambda_{HF}-\lambda_{EX}\rvert$
8	54	-5.2
18	96	-6.3
32	150	-7.2

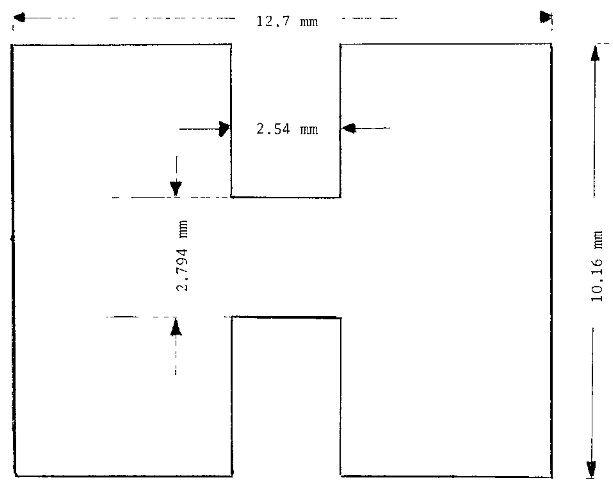

Fig. 1. Geometry of double-ridged waveguide.

VI. Numerical Examples

Two numerical examples are given: rectangular waveguide and double-ridged waveguide.

Example 1: We consider the TE problem for a rectangular waveguide with sides $a = 2$ cm and $b = 1$ cm. We compare the computed cutoff wavelengths (in cm) for Lagrangian third-order polynomials (λ_L) and Hermitian fifth-order polynomials (λ_{HI}) with imposed boundary conditions, to the exact ones (λ_{EX}). The results are compared for the TE_{10} mode and are given in Table I. The rectangle has been partitioned to several meshes with m right-angle triangles in each mesh. The order of $\tilde{\boldsymbol{T}}$ or $\tilde{\boldsymbol{S}}$ is denoted by n. One can easily observe that in the Hermitian case, low matrix dimensions give accurate results. This fact reduces computation time as well as computer memory.

Next we assume Hermitian approximation but we assume free boundary conditions. The eigenvalues so obtained are denoted by λ_{HF} and are given in Table II.

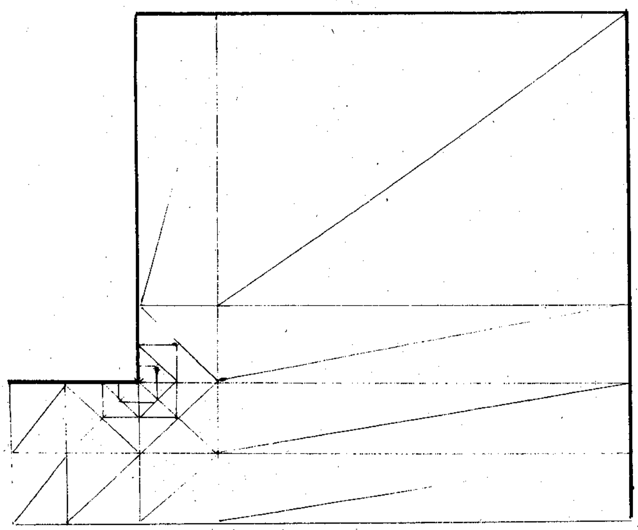

Fig. 2. Finite element refinement of a quarter double-ridged waveguide.

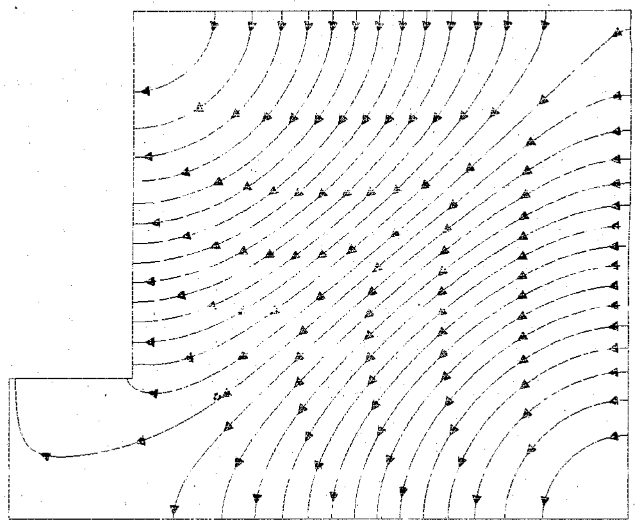

Fig. 4. Electric field lines of $TE_{20}T$ mode for a quarter double-ridged waveguide.

TABLE III
CONVERGENCE OF CUTOFF WAVELENGTH (IN MM) FOR DOUBLE-RIDGED WAVEGUIDE USING FEM WITH HERMITIAN POLYNOMIALS AND COMPARISON BETWEEN OTHER ANALYSES WITH IMPOSED BOUNDARY CONDITIONS

Mode Name	λ_{HI} n=27 m=6	n=88 m=24	n=126 m=36	n=164 m=48	from [1]	from [2]
$TE_{10}H$	42.68	43.429	43.582	43.641	43.69	43.72
$TE_{20}T$	10.137	10.145	10.146	10.147	10.11	10.15
$TE_{30}H$	9.347	9.358	9.36	9.36	9.368	9.36

H–Hybrid; T–Trough.

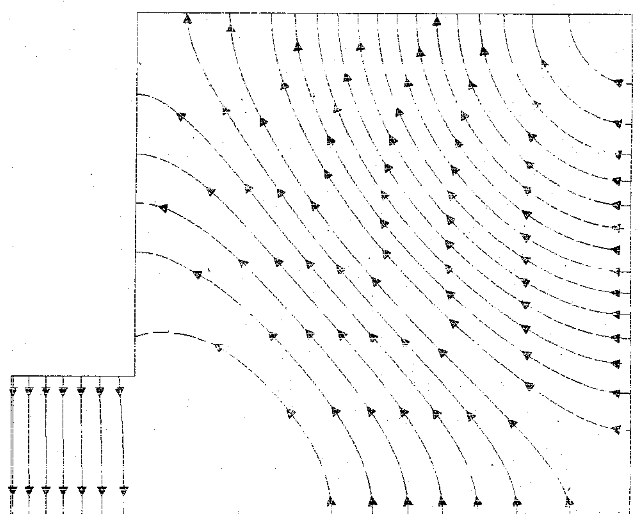

Fig. 5. Electric field lines of $TE_{30}H$ mode for a quarter double-ridged waveguide.

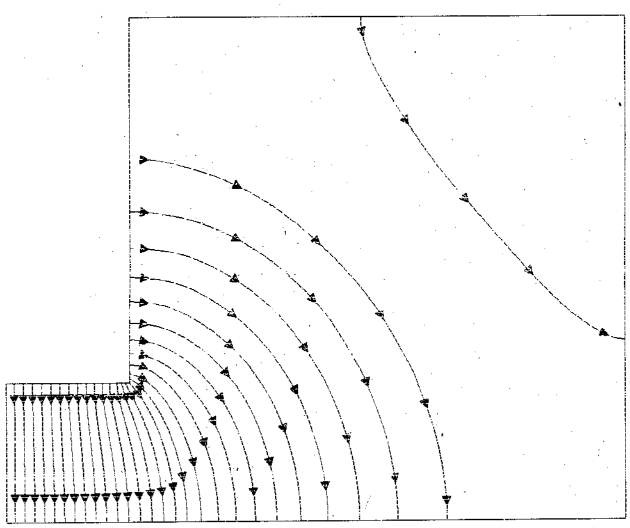

Fig. 3. Electric field lines of $TE_{10}H$ mode for a quarter double-ridged waveguide.

TABLE IV
CONVERGENCE OF CUTOFF WAVELENGTH (IN MM) FOR DOUBLE-RIDGED WAVEGUIDE USING FEM WITH HERMITIAN POLYNOMIALS WITH FREE BOUNDARY CONDITIONS

Mode Name	λ_{HF} n=37 m=6	n=108 m=24	n=150 m=36	n=192 m=48
$TE_{10}H$	42.76	43.44	43.59	43.645
$TE_{20}T$	10.138	10.145	10.147	10.147
$TE_{30}H$	9.349	9.358	9.36	9.36

H–Hybrid; T–Trough.

It may be concluded that the reduction in matrix order n when Neumann boundary conditions are imposed does not significantly decrease the eigenvalue accuracy and it is therefore convenient to impose them.

Example 2: In this second example, we consider a double-ridged waveguide whose dimensions are shown in Fig. 1. Assuming fifth-degree Hermitian polynomials with imposed boundary conditions, we follow [7] and refine the mesh near the singularity (e.g., Fig. 2). The convergence, for some modes, is demonstrated in Table III. The field lines corresponding to those modes are given for a quarter waveguide in Figs. 3–5.

In Table IV we demonstrate the convergence when free boundary conditions are assumed. By comparing Tables III and IV, it may be concluded that it is advantageous to impose the Neumann boundary conditions.

Appendix I

The Ten Hermitian Polynomials of Third Degree

$$\alpha_1 = 3p_1^2 - 7p_1p_2 - 2p_1^3 + 7p_1^2p_2 + 7p_1p_2^2$$

$$\alpha_2 = 3p_2^2 - 7p_1p_2 - 2p_2^3 + 7p_1^2p_2 + 7p_1p_2^2$$

$$\alpha_3 = 1 - 3p_1^2 - 3p_2^2 - 13p_1p_2 + 2p_1^3 + 2p_2^3 + 13p_1p_2^2 + 13p_1^2p_2$$

$$\alpha_4 = 27p_1p_2 - 27p_1^2p_2 - 27p_1p_2^2$$

$$\alpha_5 = (2p_1p_2 - 2p_1p_2^2 - 2p_1^2p_2 - p_1^2 + p_1^3)$$

$$\alpha_6 = (-p_1p_2 + p_1^2p_2 + 2p_1p_2^2)$$

$$\alpha_7 = (p_1 - 2p_1^2 + p_1^3 - 3p_1p_2 + 3p_1^2p_2 + 2p_1p_2^2)$$

$$\alpha_8 = (-p_1p_2 + p_1p_2^2 + 2p_1^2p_2)$$

$$\alpha_9 = (2p_1p_2 - p_2^2 - 2p_1^2p_2 + p_2^3 - 2p_1p_2^2)$$

$$\alpha_{10} = (p_2 - 2p_2^2 + p_2^3 - 3p_1p_2 + 3p_1p_2^2 + 2p_1^2p_2).$$

The 18 Hermitian Polynomials of Fifth degree

$$\alpha_1 = p_1^2(10p_1 - 15p_1^2 + 15p_2^2 + 6p_1^3 - 15p_2^3 - 15p_1p_2^2)$$

$$\alpha_2 = p_2^2(10p_2 - 15p_2^2 + 15p_1^2 + 6p_2^3 - 15p_1^3 - 15p_1^2p_2)$$

$$\alpha_3 = 1 - \alpha_1 - \alpha_2$$

$$\alpha_4 = p_1^2(-4p_1 + 7p_1^2 - 7.5p_2^2 - 3p_1^3 + 7.5p_1p_2^2 + 7.5p_2^3)$$

$$\alpha_5 = p_1p_2^2(3 - 2p_2 - 1.5p_1 - 1.5p_1^2 + 1.5p_1p_2)$$

$$\alpha_6 = p_1(1 - 3p_2^2 - 6p_1^2 + 8p_1^3 - 6p_1p_2^2 + 2p_2^3 - 3p_1^4 + 9p_1^2p_2^2 + 6p_1p_2^3)$$

$$\alpha_7 = p_1^2p_2(3 - 2p_1 - 1.5p_2 - 1.5p_2^2 + 1.5p_1p_2)$$

$$\alpha_8 = p_2^2(-4p_2 + 7p_2^2 - 7.5p_1^2 - 3p_2^3 + 7.5p_1^3 + 7.5p_1^2p_2)$$

$$\alpha_9 = p_2(1 - 3p_1^2 - 6p_2^2 + 8p_2^3 - 6p_1^2p_2 + 2p_1^3 - 3p_2^4 + 9p_1^2p_2^2 + 6p_1^3p_2)$$

$$\alpha_{10} = p_1^2p_2(-1 + p_1 + 0.5p_2 + 0.5p_2^2 - 0.5p_1p_2)$$

$$\alpha_{11} = p_1p_2^2(-1 + p_2 + 0.5p_1 + 0.5p_1^2 - 0.5p_1p_2)$$

$$\alpha_{12} = p_1p_2(1 - 2p_1 - 2p_2 + p_1^2 + p_2^2 + 2p_1p_2)$$

$$\alpha_{13} = p_1^2(0.5p_1 - p_1^2 + 1.25p_2^2 + 0.5p_1^3 - 1.25p_1p_2^2 - 1.25p_2^3)$$

$$\alpha_{14} = 0.25p_1^2p_2^2(1 - p_1 + p_2)$$

$$\alpha_{15} = 0.5p_1^2(1 - 3p_1 + 3p_1^2 - 3p_2^2 - p_1^3 + 2p_2^3 + 3p_1p_2^2)$$

$$\alpha_{16} = 0.25p_1^2p_2^2(1 + p_1 - p_2)$$

$$\alpha_{17} = p_2^2(0.5p_2 - p_2^2 + 1.25p_1^2 + 0.5p_2^3 - 1.25p_1^3 - 1.25p_1^2p_2)$$

$$\alpha_{18} = 0.5p_2^2(1 - 3p_2 + 3p_2^2 - 3p_1^2 - p_2^3 + 2p_1^3 + 3p_1^2p_2).$$

Appendix II

Table V–VIII give the matrices T and Q for standard triangles for third-and fifth-degree Hermitian polynomials. As the matrices are symmetric, we give only the upper triangle of T and Q^2 and the lower triangle of Q^1 and Q^3.

TABLE V
Cubic T AND Q^1 MATRICES FOR STANDARD TRIANGLE

1252	28	28	540	-212	34	34	106	-8	-26
	1252	28	540	-8	106	-26	34	-212	34
		1252	540	-8	-26	106	-26	-8	106
49			2916	-108	54	54	54	-108	54
70	199			40	-8	-8	-20	2	6
70	1	199			16	-4	10	-20	-2
-189	-270	-270	729			16	-2	6	4
-14	-20	-20	54	4			16	-8	-4
14	35	5	-54	-4	7			40	-8
14	5	35	-54	-4	1	7			16
7	22	-2	-27	-2	5	-1	7		
-14	-38	-2	54	4	-7	-1	-5	10	
0	-3	3	0	0	0	0	0	0	3

Common denominators — T: 10 080; Q^1: 90.

TABLE VI
Cubic Q^2 AND Q^3 MATRICES FOR STANDARD TRIANGLE

199	70	1	-270	-38	22	-3	35	-20	5
	49	70	-189	-14	7	0	14	-14	14
		199	-270	-2	-2	3	5	-20	35
199			729	54	-27	0	-54	54	-54
1	199			10	-5	0	-7	4	-1
70	70	49			7	0	5	-2	-1
-270	-270	-189	729			3	0	0	0
-38	-2	-14	54	10			7	-4	1
-3	3	0	0	0	3			4	-4
22	-2	7	-27	-5	0	7			7
3	-3	0	0	-3	0	0	3		
-2	-38	-14	54	1	-3	1	0	10	
-2	22	7	-27	1	0	-5	0	-5	7

Common denominator for Q^2 and Q^3: 90.

Acknowledgment

The authors wish to thank Mrs. Z. Hazan for her contribution in the programming of the computer programs involved. The authors also wish to thank Y. Kol and Dr. A. Frankel for many helpful discussions.

References

[1] Y. Utsumi, "Variational analysis of ridged waveguide modes," *IEEE Trans. Microwave Theory Tech.* vol MTT-33, pp. 111–120, Feb. 1985.
[2] J. P. Montgomery, "On the complete eigenvalue solution of ridged waveguide," *IEEE Trans. Microwave Theory Tech.* vol. MTT-19, pp. 547–555, June 1971.
[3] S. M. Saad, "Review of numerical methods for the analysis of arbitrarily shaped microwave and optical dielectric waveguides," *IEEE Trans. Microwave Theory Tech.* vol. MTT-33, pp. 894–899, Oct. 1985.
[4] P. P. Silvester and R. L. Ferrari, *Finite Elements for Electrical Engineers.* New York: Cambridge University Press, 1983.
[5] G. Strang and G. J. Fix, *An Analysis of the Finite Element Method.* Englewood Cliffs, NJ: Prentice-Hall, 1973
[6] R. Wait and A. R. Mitchell, *Finite Element Analysis and Applications.* New York: Wiley, 1985.
[7] P. Daly, "Singularities in transmission lines," in *Proc. Brunel Univ. Conf. Inst. Math. and Appl.*, 1973.

TABLE VII
Quintic T AND Q^1 MATRICES FOR STANDARD TRIANGLE

1286400	343200	429600	-320640	90360	112080	175560	-120000	56640	-34840	-21640	8360	29960	6460	10620	9460	14240	3900
	1286400	429600	-120000	175560	56640	90360	-320640	112080	-21640	-34840	8360	14240	9460	3900	6460	29960	10620
		1675200	-145440	66720	243120	66720	-145440	243120	-17440	-17440	20240	16520	2560	17160	2560	16520	17160
			88800	-30540	-36600	-49620	41328	-20208	10420	7260	-2860	-8780	-2110	-3390	-2770	-4844	-1434
				33384	11736	22848	-49620	15552	-5304	-6928	1540	3510	2064	906	1632	5010	1398
					47424	15552	-20208	31176	-3936	-3112	3520	4020	516	3744	588	2424	2076
						33384	-30540	11736	-6928	-5304	1540	5010	1632	1398	2064	3510	906
							88800	-36600	7260	10420	-2860	-4844	-2770	434	-2110	-8780	-3390
								47424	-3112	-3936	3520	2424	588	2076	516	4020	3744
									1496	1232	-396	-1090	-364	-346	-428	-830	-242
										1496	-396	-830	-428	-242	-364	-1090	-346
											352	330	66	264	66	330	264
												900	235	365	285	562	177
													142	43	122	285	53
														312	53	177	134
															142	235	43
																900	365
																	312

14400																	
-3600	410400																
-10800	-406800	417600															
-7200	1800	5400	3600														
-3240	74160	-70920	1620	17784													
-3960	-72360	76320	1980	-16164	18144												
5040	35640	-40680	-2520	10836	-13356	33984											
-7200	-91800	99000	3600	-17100	20700	-14040	41040										
5760	-51840	46080	-2880	-7416	4536	4896	4320	42624									
-1680	-5880	7560	840	-1692	2532	-5328	2760	-1632	976								
-720	-12120	12840	360	-2868	3228	-2712	4440	312	504	656							
600	-5400	4800	-300	-1020	720	660	900	3840	-220	100	480						
1200	-300	-900	-600	-270	-330	420	-600	480	-140	-60	50	100					
-840	6060	-5220	420	1674	-1254	936	-1140	-816	-112	-228	-110	-70	184				
-360	-5760	6120	180	-1404	1584	-1356	1740	336	252	288	60	-30	-114	144			
-360	4740	-4380	180	1446	-1266	2064	-1380	-384	-288	-272	-70	-30	156	-126	224		
1500	7200	-8700	-750	1320	-2070	1710	-4230	360	-370	-470	-30	125	55	-180	125	510	
660	-2940	2280	-330	-426	96	366	-330	2904	-122	-38	220	55	-61	6	-19	115	264

Common denominators — T: 13 305 600; Q^1: 604 800.

TABLE VIII
Quintic Q^2 AND Q^3 MATRICES FOR STANDARD TRIANGLE

410400	-3600	-406800	-91800	35640	-51840	74160	1800	-72360	-12120	-5880	-5400	7200	4740	-2940	6060	-300	-5760
	14400	-10800	-7200	5040	5760	-3240	-7200	-3960	-720	-1680	600	1500	-360	660	-840	1200	-360
		417600	99000	-40680	46080	-70920	5400	76320	12840	7560	4800	-8700	-4380	2280	-5220	-900	6120
			41040	-14040	4320	-17100	3600	20700	4440	2760	900	-4230	-1380	-330	-1140	-600	1740
				33984	4896	10836	-2520	-13356	-2712	-5328	660	1710	2064	366	936	420	-1356
					42624	-7416	-2880	4536	312	-1632	3840	360	-384	2904	-816	480	336
						17784	1620	-16164	-2868	-1692	-1020	1320	1446	-426	1674	-270	-1404
							3600	1980	360	840	-300	-750	180	-330	420	-600	180
								18144	3228	2532	720	-2070	-1266	96	-1254	-330	1584
									656	504	100	-470	-272	-38	-228	-60	288
										976	-220	-370	-288	-122	-112	-140	252
											480	-30	-70	220	-110	50	60
												510	125	115	55	125	-180
													224	-19	156	-30	-126
														264	-61	55	6
															184	-70	-114
																100	-30
																	144

403200																	
-331200	403200																
-72000	-72000	144000															
-88200	84600	3600	39240														
-39600	7200	32400	2700	31824													
27000	-63000	36000	-14220	5076	42624												
7200	-39600	32400	-23220	4896	11124	31824											
84600	-88200	3600	-16920	-23220	16020	2700	39240										
-63000	27000	36000	16020	11124	-24624	5076	-14220	42624									
600	7800	-8400	4080	-1932	-2748	-6348	0	-1452	1416								
7800	600	-8400	0	-6348	-1452	-1932	4080	-2748	624	1416							
-4800	-4800	9600	600	1800	2400	1800	600	2400	-480	-480	720						
6600	-7800	1200	-3930	480	1890	2940	1110	-1290	-610	-190	20	460					
-1500	300	1200	-300	1554	246	606	-1260	354	-192	-348	60	85	114				
3900	-5100	1200	-1710	-54	2904	954	1410	-2304	-218	-2	40	205	11	264			
300	-1500	1200	-1260	606	354	1554	-300	-246	-348	-192	60	175	66	29	114		
-7800	6600	1200	1110	2940	-1290	480	-3930	1890	-190	-610	20	-20	175	-125	85	460	
-5100	3900	1200	1410	954	-2304	-54	-1710	2904	-2	-218	40	-125	29	-204	11	205	264

Common denominator for Q^2 and Q^3: 604 800.

Moshe Israel (M'83) received his formal training in applied mathematics at the Weizmann Institute of Science, Rehovot, Israel, where he received the Ph.D. in 1975. From 1976 to 1978 he was a postdoctoral fellow in the Department of Geophysics at Stanford University, where he worked on computational seismology.

Since 1978 he has been with the Electromagnetics Department at RAFAEL, Haifa, Israel, where he is in charge of a Research and Development Group working on computational techniques in electromagnetics. In 1984 and 1985 he spent a sabbatical year as a Principal Engineer at the RF Technology Center at ERA, Leatherhead, England.

Ruth Miniowitz received the B.Sc., M.Sc., and D.Sc. degrees in mathematics from the Israel Institute of Technology, Haifa, Israel, in 1972, 1975, and 1978, respectively.

Between 1978 and 1983 she was a Visiting Assistant Professor in the mathematics departments of the universities of Maryland, Michigan, Kentucky, and Northern Illinois. Since 1983 she has been a Senior Researcher at RAFAEL.

Dr. Miniowitz is a member of the American Mathematical Society and the Israel Union of Mathematics.